Taylor & Francis
Taylor & Francis Group

Applied Artificial Intelligence
An International Journal

ISSN: (Print) (Online) Journal homepage: https://www.tandfonline.com/loi/uaai20

Emulating Heterogeneity of Individuals and Visualizing Its Influence on Ant Swarm Migration

Hideyasu Sasaki

To cite this article: Hideyasu Sasaki (2022) Emulating Heterogeneity of Individuals and Visualizing Its Influence on Ant Swarm Migration, Applied Artificial Intelligence, 36:1, 2138120, DOI: 10.1080/08839514.2022.2138120

To link to this article: https://doi.org/10.1080/08839514.2022.2138120

Published online: 10 Nov 2022.

APPLIED ARTIFICIAL INTELLIGENCE
2022, VOL. 36, NO. 1, e2138120 (3447 pages)
https://doi.org/10.1080/08839514.2022.2138120

Taylor & Francis
Taylor & Francis Group

Emulating Heterogeneity of Individuals and Visualizing Its Influence on Ant Swarm Migration

Hideyasu Sasaki

ICT Testbed R&D Promotion Center, National Institute of Information and Communications Technology (NICT), Koganei, Tokyo, Japan

ABSTRACT

Robot swarm can be given with different functions such as ground cruising, wall climbing, and each robot is implemented with a choice from such functions. Regarding ground mobility, findings on ant swarm in biology indicate that *Temnothorax albipennis* ant swarm including many immobile individuals accomplishes efficient migration. Our previous work revealed that 60% of active population is enough to achieve such goal and the conclusion is consistent with field studies of biologists. However, the impacts of active population ratio (active ratio) rather than species-specific elements have not been clear enough yet. Here, hypothesizing that efficient swarm migration could be generated by lowering active ratio, we removed species-specific elements from simulation and challenged particle swarm optimization (PSO) to emulate the migration and visualize global status of the swarm with simple parameter configurations. Our statistical analysis shows that the performance simulation outcomes of the algorithm are equivalent between each active-ratios of 60% and 100%. Heterogeneity of ground mobility of individuals has not put any negative impacts on efficient swarm migration. Statistical visualization of the outcomes provides the basis for evaluation of global status of swarm migration and it can lead to exploration of robot swarm migration involving functional heterogeneity of ground mobility.

ARTICLE HISTORY
Received 14 August 2022
Revised 3 October 2022
Accepted 13 October 2022

1. Introduction

Swarm migration is of interest in biology for its intelligent behavior that is often specific to each animal species (Camazine et al. 2001) and it provides many technical inspirations to the domain of swarm robotics where researchers seek to understand the functional benefits of such animal behavior and use them to have a group of robots achieve goals such as ground migration without collisions (Dorigo, Theraulaz, and Trianni 2021). Such ground migration is typically studied on ant swarm migration in behavioral biology so as robot swarm migration is investigated in robotics engineering for involvement of heterogeneity of ground mobility in behavioral function of robots. For

CONTACT Hideyasu Sasaki hsasaki@nict.go.jp ICT Testbed R&D Promotion Center, National Institute of Information and Communications Technology (NICT), 4-2-1, Nukui-Kitamachi, Koganei, Tokyo, 184-8795, Japan

example, a robot swarm is often given with different goals such as ground cruising, wall climbing, however any robot is not designed to be equipped with enough power to fulfill different functions simultaneously (Dorigo et al. 2013). In this case, cruise capability that is ground mobility in swarm migration is the key requirement on a functional heterogeneity between two different types of swarm robots. Swarm migration of *Temnothorax* (formerly *Leptothorax*) *albipennis* ant demonstrates such heterogeneous function regarding ground mobility. In the ant swarm migration some workers always contribute to the task for migration, while other workers never commit themselves to this important task for their colony and they just wait for getting carried by active ones (Dornhaus et al. 2008). This functional heterogeneity benefits the ant swarm migration dynamics for reserving inactive workers as labor force (Charbonneau, T. Sasaki, and Dornhaus 2017). Lowering active ratio of worker ants has ant colony accomplish swarm migration in an efficient manner. Findings in the ant swarm migration indicate that identifying a proper value of the active ratio of swarm robots which are equipped with ground mobility can achieve the goals of efficient cruise control for swarm migration while they drag immobile others.

Generically, most schemes of ant swarm migration are often represented in the domain of traffic flow dynamics in physics by using Cellular Automata (CA) analysis that is introduced as a kinematic approach for understanding such collective behavior (Chowdhury et al. 2002; John et al. 2008, 2009; H. Sasaki and Leung 2013). Contemporary researchers in the domain of active matter systems in physics develop a self-reinforcement protocol for learning that is inspired by ant swarm migration and it is incorporated into CA model analysis of robot swarm migration (Aguilar et al. 2018; Gravish et al. 2012, 2015; Linevich, Monaenkova, and Goldman 2016; Monaenkova et al. 2015). In the domain of swarm engineering recent studies introduce reversal functions for avoiding collisions between swarm robots (Aina et al. 2022), though each robot is assumed to be functionally identical to each other so that active ratio in swarm migration has not been discussed in any domain of studies yet. It is useful to have every robot respond to the environments and switch the functional status of ground mobility between on and off. However, such function is classified homogeneous behavioral-functionality that is compatible with inclusion of immobile constituents which are dragged by others in the swarm. We aim to find a proper value of active ratio that can have efficient ant swarm migration accomplished so as it can indicate the equivalent to such value for efficiently actuating a robot swarm of heterogeneous behavioral-functionality of ground mobility.

Our previous work revealed that *Temnothorax albipennis* ant swarm migration is more efficiently accomplished at the active ratio of 60% than the full 100% active-ratio (H. Sasaki 2019a, 2019b) and that the results of simulation work are consistent with the data obtained from the field studies reported by

Table 1. The maximum value of real-world active ratio in ant swarm migration.

Field Research	Active Ratio
Pratt (2005)	52.0–54.0% (Mean)*
Dornhaus, Holley, and Franks (2009)	56.0% (Median) - Small Population Sizes
Dornhaus, Holley, and Franks (2009)	54.0% (Median) - Large Population Sizes
Dornhaus et al. (2008)	31.0% (Median) - Small Population Sizes
Dornhaus et al. (2008)	58.0% (Median) - Large Population Sizes

* A mixture of the large and small population sizes; Pratt (2005) reports mean values and Dornhaus, Holley, and Franks (2009) and Dornhaus et al. (2008) report median values.

expert ant biologists (Dornhaus et al. 2008; Dornhaus, Holley, and Franks 2009; Pratt 2005). Table 1 provides an overview of results acquired by the field studies. The value of 60% is the equivalent to the real-world maximum value of active ratio and we particularly focused on the ant swarm migration performed at the value.

In that work, we used a metaheuristic algorithm, PSO, and included various species-specific elements such as an initial distribution of position of individual ants in the swarm for faithful reproduction of ant swarm migration. Ant swarm migration is a decentralized self-organizing system that solely relies on local information gathering in the swarm, though monitoring and visualization of global status of the swarm is mandatory for evaluating performance simulation outcomes. PSO algorithms can have the global status of swarm migration grasped statistically and visually, because they can provide not only local information gathered by individuals in a swarm but also global information aggregated by the swarm. Incorporating other decentralized algorithms for global optimization developed in the domain of evolutionary computation and involving sophisticated parameter configurations in modeling and simulation may be more beneficial to achievement of productive performance results in swarm migration. For example, another powerful metaheuristic algorithm such as the Bat algorithm with adaptive inertia weights which can accomplish Sugeno-function fuzzy search (Rauf et al. 2020) and an evolutionary algorithm such as a differential evolution algorithm for continuous optimization and classification analysis (Rauf, Bangyal, and Lali 2021) are candidates for the purpose of improving the results in simulation. Apparently, introduction of such decentralized algorithms without a clue for grasping necessary global status of swarm into modeling and simulation can only increase complexity in evaluation of performance simulation outcomes without necessary clarification to the relation of active ratio with swarm migration and would not give any answer in context discussed in this article to the problem, whether active ratio has swarm migration better-performed. Therefore, we don't use the decentralized algorithms in this article and we will remove species-specific parametric elements from algorithm formulation, and only focus on the probability relation regarding the functional heterogeneity of ground mobility that is represented by active ratio.

In the following, we summarize a description of algorithm formulation for emulating the ant swarm migration that is accomplished by individuals of behavioral functional-heterogeneity, provide a setup for performance simulation, statistically analyze performance simulation outcomes, and show that there are not any negative impacts arising from such small value of active ratio on the efficiency for swarm migration.

2. Algorithm

Our algorithm that is simplified from our previous study (H. Sasaki 2019a, 2019b) is programmed to execute emulation of ant swarm migration by using a classical PSO algorithm (Cleghorn and Engelbrecht 2018; Clerc and Kennedy 2002; Kennedy and Eberhart 1995) with parameter configurations introduced in the early period of time (Clerc and Kennedy 2002).

The algorithm has a set of computational agents in the form of random particles. Those particles are used to emulate the motion of individual constituents in an ant swarm for simulating the migration. At every iteration step, the algorithm initializes particles and the search process for an optimum solution is repeated by updating the position and velocity of particles. Once updated, the position and velocity is evaluated by using an evaluation function that is called cost function in comparison with two different types of best positions that are the personal best position of each particle and the global best position in a swarm of particles. After finding the two best positions, each value is updated for position and velocity and an optimum solution can be finally identified (Pereira 2010).

The motion parameters are evaluated with the cost function that leads to an optimum solution representing a shortest path and this path emerges when the distance traveled by individuals is minimized. In this way, the motion of individual constituents in the swarm migration can be successfully emulated to find such the best path for a new nest site for the swarm through trial and error.

The algorithm consists of two parts: active-particle update process and inactive-particle update process. First, the position and velocity of an active particle represents the individual behavior of an active worker ant. Each active particle is defined and updated in the same way that is represented in the classical PSO algorithm, as follows. The velocity $v \in R$ and position $x \in R$ of the $i \in N$-th active particle in the population size S at a discrete time step $t \in N$ (the t-th iteration step) is defined and updated through the formula:

$$v_i(t+1) = \omega v_i(t) + c_1 r_1(t)\{p_i(t) - x_i(t)\} + c_2 r_2(t)\{g(t) - x_i(t)\}, \quad (1)$$

$$x_i(t+1) = x_i(t) + v_i(t+1). \quad (2)$$

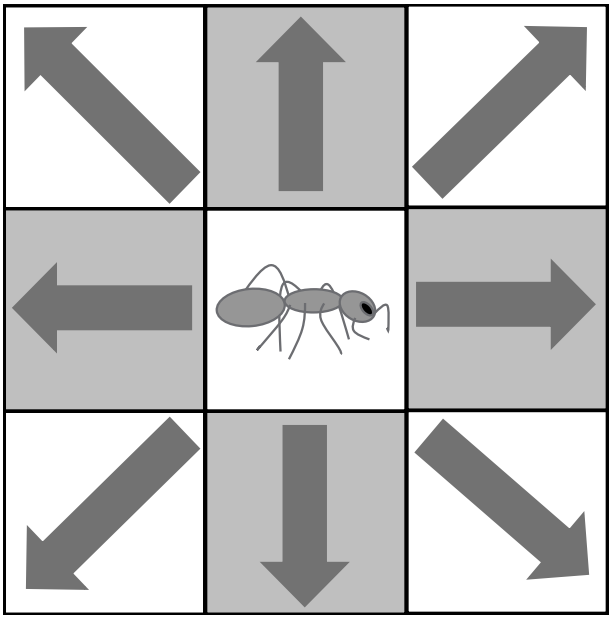

Figure 1. Particle representing a worker ant has eight two-dimensional directions of motion on land surface.

Note: random components $r_{1,k}(t)$, $r_{2,k}(t)$ $\sim U(0,1)$; the vector component k for v_i, x_i; personal (cognitive) coefficient c_1; social coefficient c_2; inertia weight ω. The vector component k of the velocity v and position x of the i-th active particle represents the direction traveled by this particle and it is defined as the value of 8 that is same with our previous work (H. Sasaki 2019a, 2019b). Each particle represents a worker ant that migrates on land surface not only travels forward and backward, but also shifts in the transverse direction, and moves and shifts at the same time so that the direction traveled by the particle is defined in a discrete form that consists of eight two-dimensional directions, i.e., $K = 8$, as shown in Figure 1.

The personal best position represents the location that each particle has visited and where it has obtained the lowest cost-function evaluation. The global best position represents the location that is the neighborhood of each particle and where a swarm including the particle has visited and obtained the lowest cost-function evaluation. The personal best position p of the i-th active particle and the global best position g at the t-th iteration step are defined and updated with the cost function f through the formula:

$$p_i(t+1) = \begin{cases} x_i(t+1) & \textbf{if } f\ (x_i(t+1)) < f\ (p_i(t)) \\ p_i(t) & \textbf{else}, \end{cases} \tag{3}$$

$$g(t+1) \;=\; \underset{p_i(t)\,\in\,P(t)}{\arg\min}\; f\;(p_i(t+1)). \tag{4}$$

The output of cost function represents the distance traveled by individual ants which search for the shortest path for a new nest site and the target point zero in the function represents this nest site. The distance takes a positive value or negative value that is measured from the target point zero so that the square of difference between these values is computed and the accumulated square of difference values should be minimized through vector component k.

Second, the position and velocity of an inactive particle represents the individual behavior of an inactive worker ant. Each inactive particle is defined and updated in a different way from the active-particle update process, as follows. The velocity v and position x of the i-th inactive particle at the t-th iteration step is defined and updated through the formula:

$$v_i(t+1) = v_{i-1}(t+1), \tag{5}$$

$$x_i(t+1) = x_{i-1}(t+1) = x_{i-1}(t) + v_i(t+1). \tag{6}$$

Note: the random components $r_{1,k}(t)$, $r_{2,k}(t)$, the vector component k, the parameters c_1, c_2, ω are same with the definition in the active-particle update process.

The personal best position p of the i-th inactive particle and the global best position g at the t-th iteration step are defined and updated with the cost function through the formula:

$$p_i(t+1) = p_{i-1}(t+1), \tag{7}$$

$$g(t+1) \;=\; p_i(t+1). \tag{8}$$

How status of mobility, active or inactive, is assigned to each particle is same with our previous work (H. Sasaki 2019a, 2019b) and active and inactive particles are assigned in a static form that is described in Table 2, according to respective active ratios of 5%, 10%, ..., 95%, and 100%. This static assignment is based on findings by ant behavioral biologists, Geraghty, Dunn, and Sanders (2007). They report that the population size of 20 is a basic unit of worker ants of the species discussed in this article. We have included this static size in algorithm formulation as a segment of particles that is divided by each range interval of 20 particles, thus each segment consists of 20 active particles and inactive ones. As is same with the real-world swarm migration of the ant species, it is formulated that within every 20 individual constituents (ants, i.e. particles) each active individual brings an almost equal number of inactive others residing closest to the active one and that the active one leads them to the target point of zero that is an optimal goal for the cost-function evaluation.

In the next section, we provide an overview of the setup for simulation.

Table 2. Status of mobility, active or inactive, is assigned to each particle for respective active ratios.

Active Ratio	Active Particle "ⓝ" & Inactive Particle "○"
5%	① ○ ○ ○ ○ ○ ○ ○ ○ ○ ○ ○ ○ ○ ○ ○ ○ ○ ○ ○
10%	① ○ ○ ○ ○ ○ ○ ○ ○ ○ ⑪ ○ ○ ○ ○ ○ ○ ○ ○ ○
15%	① ○ ○ ○ ○ ○ ○ ⑧ ○ ○ ○ ○ ○ ○ ⑮ ○ ○ ○ ○ ○
20%	① ○ ○ ○ ○ ⑥ ○ ○ ○ ○ ⑪ ○ ○ ○ ○ ⑯ ○ ○ ○ ○
25%	① ○ ○ ○ ⑤ ○ ○ ○ ⑨ ○ ○ ○ ⑬ ○ ○ ○ ⑰ ○ ○ ○
30%	① ○ ○ ○ ⑤ ○ ○ ⑧ ○ ○ ⑪ ○ ○ ○ ⑮ ○ ○ ⑱ ○ ○
35%	① ○ ○ ④ ○ ○ ⑦ ○ ○ ⑩ ○ ○ ⑬ ○ ○ ⑯ ○ ○ ⑲ ○
40%	① ○ ○ ④ ○ ⑥ ○ ○ ⑨ ○ ⑪ ○ ○ ⑭ ○ ⑯ ○ ○ ⑲ ○
45%	① ○ ○ ④ ○ ○ ⑦ ○ ⑨ ○ ⑪ ○ ⑬ ○ ⑮ ○ ⑰ ○ ⑲ ○
50%	① ○ ③ ○ ⑤ ○ ⑦ ○ ⑨ ○ ⑪ ○ ⑬ ○ ⑮ ○ ⑰ ○ ⑲ ○
55%	① ② ○ ④ ⑤ ○ ⑦ ○ ⑨ ○ ⑪ ○ ⑬ ○ ⑮ ○ ⑰ ○ ⑲ ○
60%	① ○ ③ ○ ⑤ ⑥ ○ ⑧ ○ ⑩ ⑪ ○ ⑬ ○ ⑮ ⑯ ○ ⑱ ○ ⑳
65%	① ② ○ ④ ⑤ ○ ⑦ ⑧ ○ ⑩ ⑪ ○ ⑬ ⑭ ○ ⑯ ⑰ ○ ⑲ ○
70%	① ② ③ ○ ⑤ ⑥ ○ ⑧ ⑨ ○ ⑪ ⑫ ⑬ ○ ⑮ ⑯ ○ ⑱ ⑲ ○
75%	① ② ③ ○ ⑤ ⑥ ⑦ ○ ⑨ ⑩ ⑪ ○ ⑬ ⑭ ⑮ ○ ⑰ ⑱ ⑲ ○
80%	① ② ③ ④ ○ ⑥ ⑦ ⑧ ⑨ ○ ⑪ ⑫ ⑬ ⑭ ○ ⑯ ⑰ ⑱ ⑲ ○
85%	① ② ③ ④ ⑤ ⑥ ○ ⑧ ⑨ ⑩ ⑪ ⑫ ⑬ ○ ⑮ ⑯ ⑰ ⑱ ⑲ ○
90%	① ② ③ ④ ⑤ ⑥ ⑦ ⑧ ⑨ ○ ⑪ ⑫ ⑬ ⑭ ⑮ ⑯ ⑰ ⑱ ⑲ ○
95%	① ② ③ ④ ⑤ ⑥ ⑦ ⑧ ⑨ ⑩ ⑪ ⑫ ⑬ ⑭ ⑮ ⑯ ⑰ ⑱ ⑲ ○
100%	① ② ③ ④ ⑤ ⑥ ⑦ ⑧ ⑨ ⑩ ⑪ ⑫ ⑬ ⑭ ⑮ ⑯ ⑰ ⑱ ⑲ ⑳

3. Simulation

A simulation setup is different from faithful reproduction of the ant swarm migration of the discussed species. From our previous work (H. Sasaki 2019a, 2019b) we removed species-specific initial distribution of position of ants, distance measure, network topology. We instead introduced a uniform probability distribution measured by the Euclid distance between individual particles with a random network topology where all particles are connected in a random fashion. Efficacy for such formulation is demonstrated in not only simplification but also direct assessments of the impacts from behavioral functional-heterogeneity of individuals on global status of the ant swarm migration. Eliminating any effect of species-specific parametric elements on performance simulation outcomes allows us to evaluate the influence of

Table 3. The definition of cost functions with values of search-range.

Cost Function		Search Range
Sphere Function	$f(x_i^k(t)) = \sum_{i\in S}\sum_{k\in K} \|\|x_i^k(t)\|\|^2$	[−5, 5]
Shifted-Schwefel's Problem 1.2	$f(x_i^k(t)) = \sum_{i\in S}\sum_{k\in K} (\sum_{j=1}^{k} x_i^k(t))^2$	[−32, 32]
Shifted-elliptic Function	$f(x_i^k(t)) = \sum_{i\in S}\sum_{k\in K} 10^{6\frac{i-1}{K-1}}\{x_i^k(t)\}^2$	[−100, 100]
Shifted-Rosenbrock's Function	$f(x_i^k(t)) = \sum_{i\in S}\sum_{k\in K-1}[100(\{x_i^k(t)\}^2 - x_i^{k+1}(t))^2 + (x_i^k(t)-1)^2]$	[−5, 5]
Shifted-Ackley's Function	$f(x_i^k(t)) = \sum_{i\in S}[-20\exp(-0.2\sqrt{\frac{1}{K}\sum_{k\in K}\{x_i^k(t)\}^2}) - \exp(\frac{1}{K}\sum_{k\in K}\cos(2\pi x_i^k(t))) + 20 + exp]$	[−32, 32]
Shifted-Rastrigin's Function	$f(x_i^k(t)) = \sum_{i\in S}\sum_{k\in K}[\{x_i^k(t)\}^2 - 10\cos(2\pi x_i^k(t)) + 10]$	[−5, 5]

$\|\cdot\|$ denotes the Euclidean norm.

heterogeneity of ground mobility between active individuals and inactive ones on the ant swarm migration by a single factor related to the mobility that is active ratio.

Newly included cost functions in the simulation setup have each search-range defined as narrow as possible and it is different from what is often used for benchmark assessments. By narrowing the range, each process of performance evaluation of the algorithm can be accelerated without losing any quality of performance simulation outcomes. A set of six cost-functions is listed in Table 3 and they have been chosen for the purpose of performance simulation and evaluation from the list of functions recommended by the series of IEEE CEC benchmark competitions (Li et al. 2013). Among the functions, three functions have search-range that is narrower than others and such narrow range eases the computational process of performance simulation for saving time. This definition of each search-range is acceptable for the purpose of performance simulation, because computing time for each process in simulation is being calibrated at a maximum number of iteration steps. The maximum number remains the same through the entire simulation process and it takes a large enough value of 3×10^6 that is chosen in reference to the benchmark competition series. Therefore, we would not calculate the duration of performance testing.

Table 4. The parameter setting of parametric values in simulation for the algorithm.

Symbol	Parameter	Default Values
S	Population Size	[20–400]
c_1	Personal (Cognitive) Coefficient	2.05
c_2	Social Coefficient	2.05
ω	Starting Value of the Inertia Weight	0.729
χ	Constriction Coefficient	0.729
φ	Multiplier for Random Numbers	4.1
v_{max}	Maximum Value of the Velocity (Step Size)	$0.2(x_{max} - x_{min})$

X is the constriction factor (Kennedy 2003); It is derived analytically through the formula given by Clerc and Kennedy (2002): $c_1 = \chi\varphi_1, c_2 = \chi\varphi_2$, $\omega = \chi = 2\kappa/|2 - \varphi - \sqrt{(\varphi^2 - 4\varphi)}|$, where $\kappa = 1$, $\varphi = \varphi_1 + \varphi_2$, and $\varphi_1 = \varphi_2 = 2.05$.

Table 4 provides a concise overview of parameter setting of parametric values in simulation for the algorithm, including the personal (cognitive) coefficient, social coefficient, inertia weight, in reference to the work by Clerc and Kennedy (2002) and Yarpiz Team (2015).

As is same with our previous work (H. Sasaki 2019a, 2019b), the range of population size *S* takes the maximum value of 400 and minimum value of 20 in reference to the population size of the real-world worker ant swarm of the *Temnothorax albipennis* species, exactly (Geraghty, Dunn, and Sanders 2007) and this species-specific element has been only retained for simulation purpose in this article. And, the simulation process was performed 50 times with the respective population sizes.

The algorithm has been implemented by using the PySwarms package ver. 1.1.0 developed by Miranda (2019) that is encoded in Python and is provided as a package for evolutionary optimization solutions. The entire simulation has been done on a Windows 10 Pro (64-bit) laptop PC that is equipped with a Core i7–7700 3.6 GHz quad-core processor with 16 GB of RAM.

The performance simulation outcomes have been evaluated by using a metrics that is called "discrepancy" and this metrics quantifies the influence of heterogeneity between individuals on global status of a swarm. Garnier et al. (2008) proposed this metrics and they ensured a successful emulation of a swarm of robots behaving like real-world cockroaches. They validated the discrepancy that was defined by quantitative difference between performance simulation outcomes (emulation of robots) and the target phenomena (aggregation of real-world cockroaches) as negligible. We follow their discrepancy

Table 5. The performance simulation outcomes between the pair of each active-ratios of 60% and 100%.

		Global Best - Mean (S.D.)	
Cost Function	Population Size	Active Ratio of 60%	Active Ratio of 100%
Sphere Function	Entire	**4.15e-02** (2.09e-02)	4.16e-02 (2.10e-02)
	Small	**9.87e-02** (5.16e-02)	9.88e-02 (5.18e-02)
	Large	**2.61e-02** (1.25e-02)	2.62e-02 (1.26e-02)
Shifted-Schwefel's Problem 1.2	Entire	**8.11e + 00** (4.59e + 00)	8.15e + 00 (4.64e + 00)
	Small	**2.02e + 01** (1.19e + 01)	2.03e + 01 (1.23e + 01)
	Large	**4.84e + 00** (2.58e + 00)	4.85e + 00 (2.54e + 00)
Shifted-elliptic Function	Entire	1.67e + 01 (8.44e + 00)	**1.67e + 01** (8.36e + 00)
	Small	**3.94e + 01** (2.10e + 01)	3.95e + 01 (2.05e + 01)
	Large	1.05e + 01 (5.02e + 00)	**1.05e + 01** (5.04e + 00)
Shifted-Rosenbrock's Function	Entire	1.24e + 01 (7.55e + 00)	**1.24e + 01** (7.43e + 00)
	Small	2.27e + 01 (1.83e + 01)	**2.25e + 01** (1.70e + 01)
	Large	**9.62e + 00** (4.65e + 00)	9.68e + 00 (4.79e + 00)
Shifted-Ackley's Function	Entire	3.16e + 00 (5.04e-01)	**3.16e + 00** (5.01e-01)
	Small	4.16e + 00 (6.92e-01)	**4.16e + 00** (6.73e-01)
	Large	2.89e + 00 (4.53e-01)	**2.89e + 00** (4.54e-01)
Shifted-Rastrigin's Function	Entire	2.01e + 01 (2.03e + 01)	**2.01e + 01** (5.92e + 00)
	Small	2.68e + 01 (2.79e + 01)	**2.66e + 01** (7.34e + 00)
	Large	**1.83e + 01** (1.82e + 01)	1.83e + 01 (5.53e + 00)

S.D. represents standard deviation; Values in **bold** are smaller than others and indicate better performance between the pair of each active-ratios.

Table 6. The distribution of discrepancy between the pair of each active-ratios in the form of percentage.

	Distribution of Discrepancy (%)	
Cost Function	Maximum	Minimum
Sphere Function	50	−20
Shifted-Schwefel's Problem 1.2	30	−30
Shifted-elliptic Function	40	−30
Shifted-Rosenbrock's Function	40	−60
Shifted-Ackley's Function	50	−40
Shifted-Rastrigin's Function	30	−40

Values indicate the maximum value and minimum value of distribution of discrepancy, while each result is better performed at the active ratio of 60% than the full 100% active-ratio performance with respective cost functions.

approach and scale the discrepancy metrics by difference of performance simulation outcomes between the pair of each active-ratios of 60% and 100%, and evaluate the influence of heterogeneity of individuals that is represented by active ratio on global status of a swarm of individuals. Once a statistical test validates such discrepancy as is negligible, performance simulation outcomes with those active ratios can be considered identical to each other. This means that extreme heterogeneity of ground mobility of individuals including inactive ones would not have any negative impacts on global status of a swarm migration.

Results of performance simulation are aggregated as the average global-best position (global best) that is acquired by averaging performance simulation outcomes of the programs implemented by using the algorithm for simulation with the set of six cost functions for respective population sizes. The global-best values indicate the superiority of performance simulation for the algorithm. And, a quantitative analysis of the discrepancy of global-best values between the pair of each active-ratios of 60% and 100% provides statistical information for visualizing performance simulation outcomes for evaluation of global status of a swarm of individuals in migration.

In the next section, we present a detailed description of the results of performance simulation for the algorithm.

4. Results

Table 5 presents a summary of performance simulation outcomes with the respective cost functions. The discrepancy of global-best values has fallen within the value of 0.1 over the outcomes recorded in the entire population sizes (20–400) and large population sizes (101–400), except for results with the two functions in the small population sizes (20–100).

Table 6 provides a summary of more detailed analysis of the same outcomes and summing each result that is better performed at the active ratio of 60% than the full 100% active-ratio performance indicates distribution of

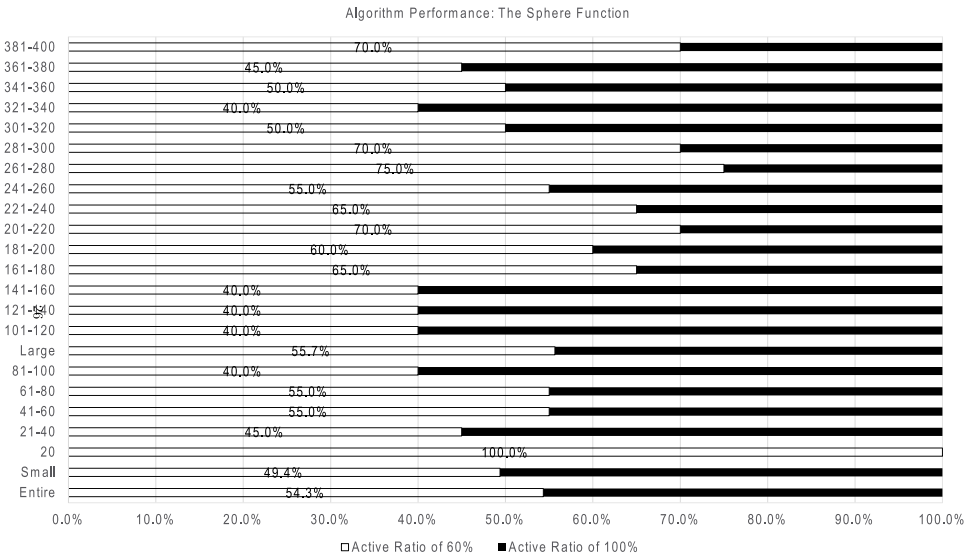

Figure 2. The performance simulation outcomes with the sphere function between the pair of each active-ratios across the entire population sizes, small population sizes, large population sizes, and each range interval of 20 population sizes. Each value indicates percentage of each result of simulation that is better performed at the active ratio of 60% than the full 100% active-ratio performance; The range of values takes the maximum value of 50% (such as the population size of 261–280) and minimum value of -20% (such as the population size of 81–100) across each range interval of 20 population sizes; The population size of 20 is a basic unit of worker ants of the species in migration (Geraghty, Dunn, and Sanders 2007).

discrepancy in the form of percentage. The range of the distribution takes the maximum value of 50% and minimum value of −60% and it is very sporadic throughout the results so that further analysis is required to obtain persuasive evidence for any conclusion. The complete results are available in Figures 2–7.

Statistical testing is expected to provide such evidence for evaluating the outcomes and understanding the influence of heterogeneity that is represented by the active ratio of 60%. We compare the mean of global-best values by using the one-tailed *t*-test (two-sample equality assuming equal/unequal variances) and the one-tailed *F*-test (two-sample variances). Here, the null hypothesis assumes that each global-best value acquired at the active ratio of 60% is equal to each global-best value acquired at the full 100% active-ratio with respective population sizes. Table 7 provides a summary of statistical-testing results of the outcomes. Summing each result that is better performed at the active ratio of 60% than the full 100% active-ratio performance across the entire population sizes (20–400) in the following significance levels indicates distribution of statistically-significant discrepancy in the form of percentage. The range of the distribution takes the maximum value of 8.66% and minimum value of 5.25% (significance level: $\alpha = 0.05$), the maximum value of 1.84% and minimum value of 0.262% ($\alpha = 0.005$), and the maximum value of 0.262% and minimum

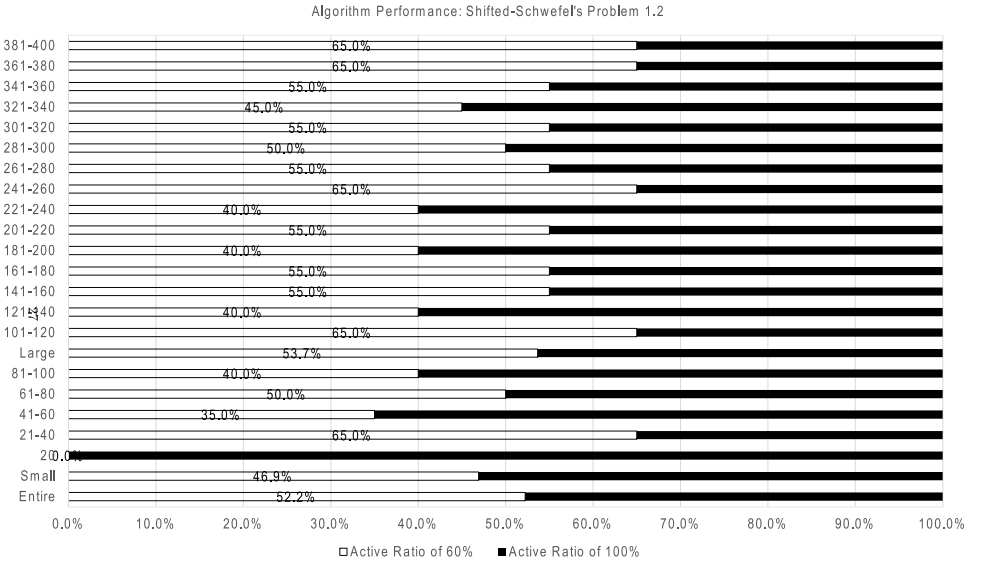

Figure 3. The performance simulation outcomes with the shifted-Schwefel's problem 1.2 between the pair of each active-ratios across the entire population sizes, small population sizes, large population sizes, and each range interval of 20 population sizes. Each value indicates percentage of each result of simulation that is better performed at the active ratio of 60% than the full 100% active-ratio performance; The range of values takes the maximum value of 30% (such as the population size of 101–120) and minimum value of -30% (such as the population size of 41–60) across each range interval of 20 population sizes; The population size of 20 is a basic unit of worker ants of the species in migration (Geraghty, Dunn, and Sanders 2007).

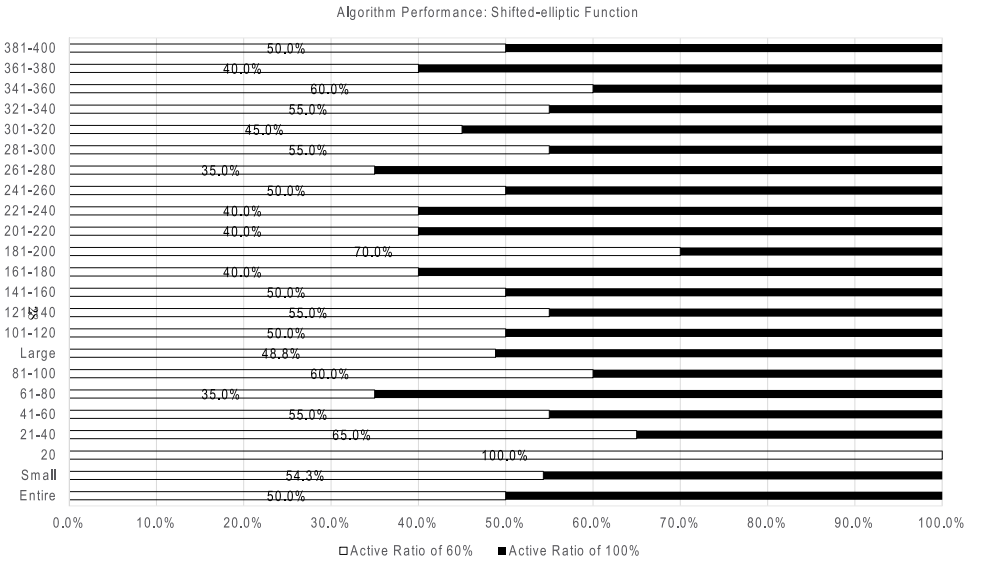

Figure 4. The performance simulation outcomes with the shifted-elliptic function between the pair of each active-ratios across the entire population sizes, small population sizes, large population sizes, and each range interval of 20 population sizes. Each value indicates percentage of each result of simulation that is better performed at the active ratio of 60% than the full 100% active-ratio performance; The range of values takes the maximum value of 40% (such as the population size of 181–200) and minimum value of -30% (such as the population size of 61–80) across each range interval of 20 population sizes; The population size of 20 is a basic unit of worker ants of the species in migration (Geraghty, Dunn, and Sanders 2007).

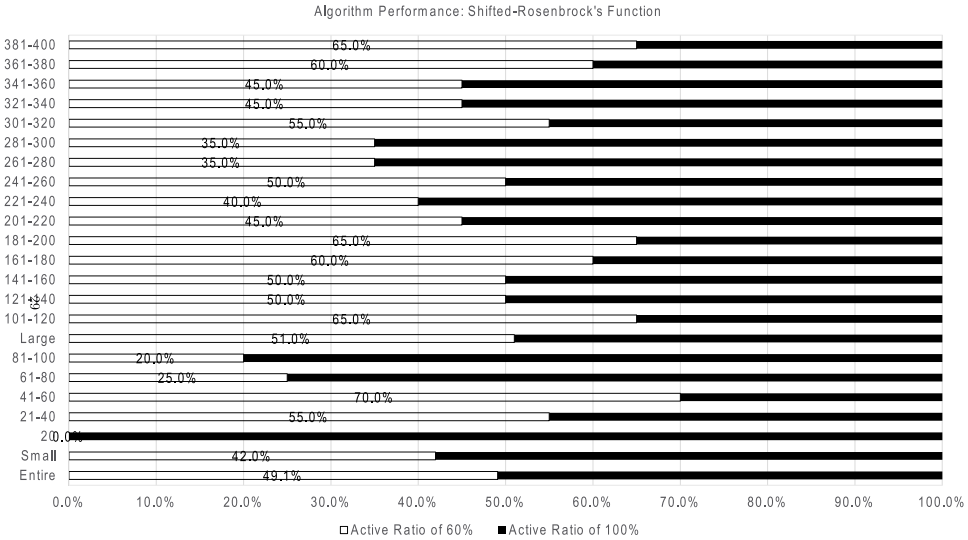

Figure 5. The performance simulation outcomes with the shifted-Rosenbrock's function between the pair of each active-ratios across the entire population sizes, small population sizes, large population sizes, and each range interval of 20 population sizes. Each value indicates percentage of each result of simulation that is better performed at the active ratio of 60% than the full 100% active-ratio performance; The range of values takes the maximum value of 40% (such as the population size of 41–60) and minimum value of -60% (such as the population size of 81–100) across each range interval of 20 population sizes; The population size of 20 is a basic unit of worker ants of the species in migration (Geraghty, Dunn, and Sanders 2007).

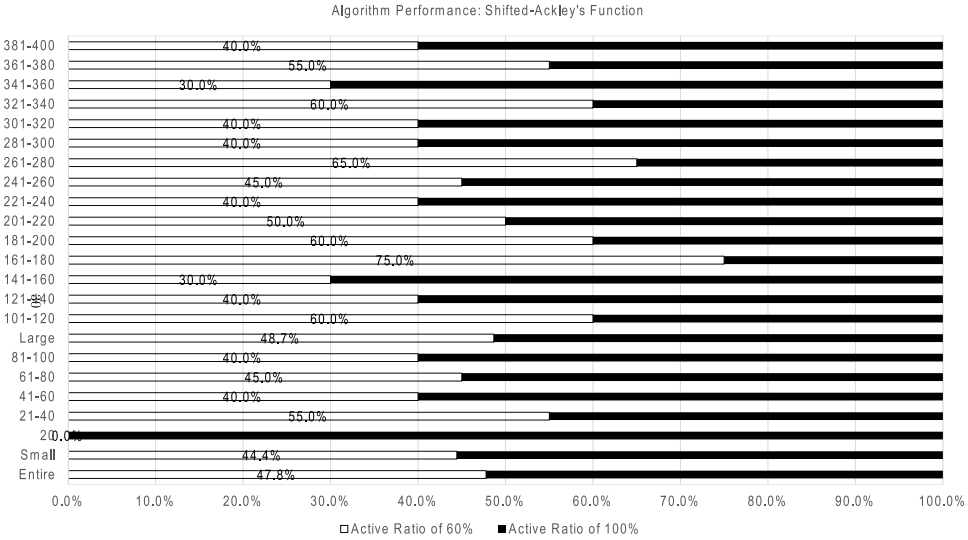

Figure 6. The performance simulation outcomes with the shifted-Ackley's function between the pair of each active-ratios across the entire population sizes, small population sizes, large population sizes, and each range interval of 20 population sizes. Each value indicates percentage of each result of simulation that is better performed at the active ratio of 60% than the full 100% active-ratio performance; The range of values takes the maximum value of 50% (such as the population size of 161–180) and minimum value of -40% (such as the population size of 141–160) across each range interval of 20 population sizes; The population size of 20 is a basic unit of worker ants of the species in migration (Geraghty, Dunn, and Sanders 2007).

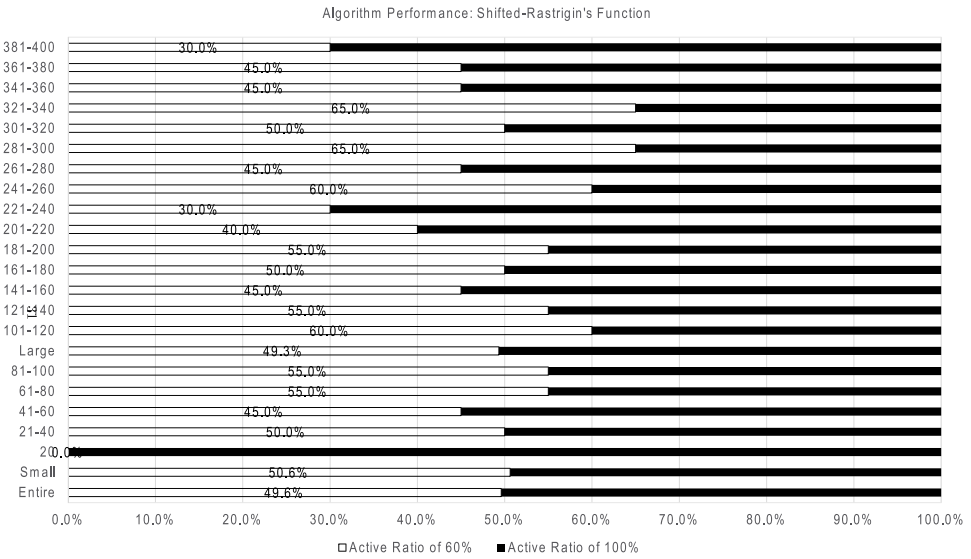

Figure 7. The performance simulation outcomes with the shifted-Rastrigin's function between the pair of each active-ratios across the entire population sizes, small population sizes, large population sizes, and each range interval of 20 population sizes. Each value indicates percentage of each result of simulation that is better performed at the active ratio of 60% than the full 100% active-ratio performance; The range of values takes the maximum value of 30% (such as the population size of 281–300) and minimum value of -40% (such as the population size of 221–240) across each range interval of 20 population sizes; The population size of 20 is a basic unit of worker ants of the species in migration (Geraghty, Dunn, and Sanders 2007).

value of 0.00% ($\alpha = 0.0005$), respectively. This analysis validates that the statistically-significant discrepancy can be considered as negligible between the pair of each active-ratios so that heterogeneity of ground mobility that is represented by the active ratio of 60% doesn't have any negative impacts on global status of a swarm of individuals in migration. The complete statistical-testing results including *t*-statics, *p*-value, and standard deviation are available in Tables 8–13.

Table 7. The distribution of statistically-significant discrepancy between the pair of each active-ratios in the form of percentage.

Cost Function	Distribution of Statistically Significant Discrepancy (%)		
α	0.05	0.005	0.0005
Sphere Function	5.77	0.525	0.262
Shifted-Schwefel's Problem 1.2	5.25	0.525	0.262
Shifted-elliptic Function	5.25	0.525	0.000
Shifted-Rosenbrock's Function	5.51	0.262	0.000
Shifted-Ackley's Function	8.66	1.84	0.000
Shifted-Rastrigin's Function	7.61	0.262	0.000

α indicates significance level; Values indicate the maximum value and minimum value of distribution of statistically-significant discrepancy, while each result is better performed at the active ratio of 60% than the full 100% active-ratio performance with respective cost functions at the respective significance levels of 0.05, 0.005, and 0.0005.

Table 8. This excerpt from the complete list of the results of simulation that is performed with the sphere function displays the global-best value that is statistically significant.

Population Size	Global Best - Mean (S.D.)		*T*-Statistics	*P*-Value
	Active Ratio of 60%	Active Ratio of 100%		
23	2.31e-01 (1.08e-01)	**1.88e-01** ∗ (9.16e-02)	2.115	0.0185
46	**8.68e-02** ∗ (3.69e-02)	1.06e-01 (5.47e-02)	2.076	0.0205
67	7.82e-02 (3.94e-02)	**6.47e-02** ∗ (3.81e-02)	1.778	0.0393
80	**5.92e-02** ∗ (3.07e-02)	7.62e-02 (5.86e-02)	2.007	0.0240
81	6.84e-02 (3.46e-02)	**5.41e-02** ∗ (6.23e-02)	2.241	0.0136
92	6.00e-02 (2.80e-02)	**4.95e-02** ∗ (2.04e-02)	2.072	0.0206
93	**4.76e-02** ∗ (2.28e-02)	5.76e-02 (2.54e-02)	2.054	0.0213
104	**4.22e-02** ∗ (2.14e-02)	5.44e-02 (3.05e-02)	2.368	0.0101
116	5.35e-02 (2.63e-02)	**4.20e-02** ∗ (2.17e-02)	2.362	0.0101
147	4.29e-02 (1.91e-02)	**3.50e-02** ∗ (1.52e-02)	2.247	0.0134
156	3.59e-02 (1.66e-02)	**3.07e-02** ∗ (1.58e-02)	1.750	0.0416
157	3.68e-02 (1.48e-02)	**2.77e-02** ∗∗∗ (1.37e-02)	3.504	0.000349
166	**2.73e-02** ∗ (1.31e-02)	3.38e-02 (1.63e-02)	2.200	0.0151
182	**2.51e-02** ∗∗ (1.17e-02)	3.39e-02 (1.56e-02)	3.068	0.00143
195	3.11e-02 (1.27e-02)	**2.46e-02** ∗ (1.25e-02)	2.563	0.00596
234	2.74e-02 (1.26e-02)	**2.21e-02** ∗ (1.00e-02)	2.305	0.0117
241	2.54e-02 (1.16e-02)	**2.13e-02** ∗ (8.53e-03)	1.866	0.0327
264	2.60e-02 (1.29e-02)	**2.00e-02** ∗ (9.23e-03)	2.517	0.00683
325	2.15e-02 (1.15e-02)	**1.66e-02** ∗ (6.82e-03)	2.542	0.00650
366	**1.53e-02** ∗ (5.96e-03)	1.81e-02 (7.05e-03)	2.107	0.0188
393	1.82e-02 (8.11e-03)	**1.45e-02** ∗ (6.70e-03)	2.470	0.00763
394	**1.42e-02** ∗ (6.62e-03)	1.74e-02 (8.66e-03)	2.037	0.0222

Among the entire population sizes of 20–400, 5.77% (22/381) of the results show significant discrepancy between the pair of each active-ratios at the significance level of 0.05, so as 0.525% (2/381) of the results at the significance level of 0.005, and 0.262% (1/381) of the results at the significance level of 0.0005. Here, values in **bold** show better performance that is acquired at each active ratio and they are measured in the form of mean value in respective population sizes, while each value that is denoted with asterisk is statistically significant at the significance level of 0.05 that is denoted by *, 0.005 that is denoted by **, and 0.0005 that is denoted by ***, in the one-tailed *t*-test. A value of standard deviation (S.D.), *t*-statistics, and *p*-value are provided for each value.

In the next section, we discuss the results of performance simulation, and give insights to understanding the heterogeneity of individuals regarding the mobility and its influence on global status of the ant swarm migration.

5. Discussion

We used the discrepancy metrics and demonstrated quantitative validation of the performance simulation outcomes and statistical testing of the outcomes showed that the ant swarm migration was successfully emulated by using the classical PSO algorithm with simple parameter configurations. This metaheuristic algorithm repeatedly updates the position and velocity of individuals and through local information gathering between individuals the global-best value emerges from iteration steps so that global status of a swarm can be visualized for understanding the heterogeneity of individuals regarding ground mobility that is represented by active ratio and its influence on global status of a swarm migration.

Apparently, it is different from faithful reproduction of the ant swarm migration that is a decentralized self-organizing system of complexity. However, inclusion of all implementation requirements which are

Table 9. This excerpt from the complete list of the results of simulation that is performed with the shifted-Schwefel's problem 1.2 displays the global-best value that is statistically significant.

Population Size	Global Best - Mean (S.D.)		*T*-Statistics	*P*-Value
	Active Ratio of 60%	Active Ratio of 100%		
33	**2.78e + 01** ∗ (1.71e + 01)	3.65e + 01 (2.35e + 01)	2.039	0.0223
41	2.67e + 01 (1.45e + 01)	**2.08e + 01** ∗ (1.18e + 01)	2.174	0.0161
42	2.72e + 01 (1.46e + 01)	**2.00e + 01** ∗ (1.32e + 01)	2.365	0.0100
50	**1.89e + 01** ∗ (1.05e + 01)	2.38e + 01 (1.74e + 01)	1.686	0.0479
53	2.06e + 01 (1.24e + 01)	**1.58e + 01** ∗ (7.78e + 00)	2.269	0.0130
93	1.25e + 01 (8.21e + 00)	**9.57e + 00** ∗ (3.83e + 00)	2.198	0.0152
149	**5.72e + 00** ∗ (3.14e + 00)	7.08e + 00 (3.29e + 00)	1.989	0.0248
155	6.66e + 00 (3.82e + 00)	**6.32e + 00** ∗ (2.85e + 00)	2.198	0.0157
156	**6.15e + 00** ∗ (3.07e + 00)	7.46e + 00 (4.04e + 00)	1.761	0.0407
157	**5.27e + 00** ∗ ∗ ∗ (2.36e + 00)	7.55e + 00 (3.95e + 00)	3.431	0.000483
158	**5.72e + 00** ∗ (3.67e + 00)	7.20e + 00 (4.07e + 00)	2.185	0.0156
172	**5.02e + 00** ∗ (2.88e + 00)	6.37e + 00 (2.43e + 00)	2.551	0.00616
213	**4.06e + 00** ∗ (2.38e + 00)	5.36e + 00 (2.94e + 00)	2.293	0.0120
229	**4.09e + 00** ∗ (1.91e + 00)	5.18e + 00 (2.90e + 00)	2.037	0.0224
242	5.02e + 00 (2.63e + 00)	**3.97e + 00** ∗ (1.78e + 00)	2.106	0.0191
265	4.76e + 00 (2.46e + 00)	**3.75e + 00** ∗ (1.91e + 00)	2.043	0.0219
276	4.26e + 00 (2.37e + 00)	**3.34e + 00** ∗ (1.81e + 00)	2.105	0.0189
300	**2.99e + 00** ∗ (1.74e + 00)	3.72e + 00 (1.57e + 00)	2.160	0.0166
346	3.41e + 00 (1.59e + 00)	**2.59e + 00** ∗ ∗ (1.41e + 00)	2.894	0.00235
370	**2.89e + 00** ∗ (1.35e + 00)	3.57e + 00 (1.88e + 00)	2.153	0.0171

Among the entire population sizes of 20–400, 5.25% (20/381) of the results show significant discrepancy between the pair of each active-ratios at the significance level of 0.05, so as 0.525% (2/381) of the results at the significance level of 0.005, and 0.262% (1/381) of the results at the significance level of 0.0005. Here, values in **bold** show better performance that is acquired at each active ratio and they are measured in the form of mean value in respective population sizes, while each value that is denoted with asterisk is statistically significant at the significance level of 0.05 that is denoted by *, 0.005 that is denoted by **, and 0.0005 that is denoted by ***, in the one-tailed *t*-test. A value of standard deviation (S.D.), *t*-statistics, and *p*-value are provided for each value.

Table 10. This excerpt from the complete list of the results of simulation that is performed with the shifted-elliptic function displays the global-best value that is statistically significant.

Population Size	Global Best - Mean (S.D.)		*T*-Statistics	*P*-Value
	Active Ratio of 60%	Active Ratio of 100%		
23	**6.82e + 01** ∗ (3.50e + 01)	8.44e + 01 (4.48e + 01)	1.932	0.0282
51	**3.57e + 01** ∗ (1.87e + 01)	4.20e + 01 (1.85e + 01)	1.848	0.0339
53	4.10e + 01 (2.10e + 01)	**3.20e + 01** ∗ (2.06e + 01)	2.059	0.0211
69	3.20e + 01 (1.78e + 01)	**2.37e + 01** ∗ ∗ (1.29e + 01)	2.640	0.00492
74	3.25e + 01 (1.67e + 01)	**2.57e + 01** ∗ (1.12e + 01)	2.520	0.00680
75	2.91e + 01 (1.59e + 01)	**2.26e + 01** ∗ (1.01e + 01)	2.318	0.0115
81	2.93e + 01 (1.61e + 01)	**2.17e + 01** ∗ ∗ (1.08e + 01)	2.642	0.00491
133	2.10e + 01 (1.14e + 01)	**1.65e + 01** ∗ (1.04e + 01)	2.434	0.00840
168	1.48e + 01 (8.06e + 00)	**1.15e + 01** ∗ (4.48e + 00)	2.623	0.00528
174	1.38e + 01 (6.13e + 00)	**1.12e + 01** ∗ (4.84e + 00)	2.393	0.00932
188	1.33e + 01 (5.92e + 00)	**1.06e + 01** ∗ (4.94e + 00)	2.439	0.00827
192	1.30e + 01 (6.11e + 00)	**1.04e + 01** ∗ (4.12e + 00)	2.294	0.0121
212	**9.74e + 00** ∗ (4.19e + 00)	1.21e + 01 (6.34e + 00)	2.149	0.0173
264	1.10e + 01 (4.88e + 00)	**8.94e + 00** ∗ (4.46e + 00)	2.021	0.0230
265	**8.14e + 00** ∗ (3.96e + 00)	1.01e + 01 (4.29e + 00)	2.332	0.0109
270	**7.79e + 00** ∗ (2.81e + 00)	9.25e + 00 (4.29e + 00)	2.063	0.0211
283	**7.46e + 00** ∗ (3.29e + 00)	9.09e + 00 (4.23e + 00)	1.945	0.0273
325	7.75e + 00 (3.17e + 00)	**6.50e + 00** ∗ (2.90e + 00)	1.915	0.0292
388	**6.13e + 00** ∗ (2.92e + 00)	7.33e + 00 (2.92e + 00)	1.804	0.0372
390	7.90e + 00 (4.09e + 00)	**6.39e + 00** ∗ (2.76e + 00)	2.181	0.0160

Among the entire population sizes of 20–400, 5.25% (20/381) of the results show significant discrepancy between the pair of each active-ratios at the significance level of 0.05, so as 0.525% (2/381) of the results at the significance level of 0.005, and 0.00% (0/381) of the results at the significance level of 0.0005. Here, values in **bold** show better performance that is acquired at each active ratio and they are measured in the form of mean value in respective population sizes, while each value that is denoted with asterisk is statistically significant at the significance level of 0.05 that is denoted by *, 0.005 that is denoted by **, and 0.0005 that is denoted by ***, in the one-tailed *t*-test. A value of standard deviation (S.D.), *t*-statistics, and *p*-value are provided for each value.

Table 11. This excerpt from the complete list of the results of simulation that is performed with the shifted-Rosenbrock's function displays the global-best value that is statistically significant.

Population Size	Global Best - Mean (S.D.)		*T*-Statistics	*P*-Value
	Active Ratio of 60%	Active Ratio of 100%		
24	**3.21e + 01** ∗ (2.20e + 01)	4.72e + 01 (4.32e + 01)	2.114	0.0190
26	**3.02e + 01** ∗∗ (1.99e + 01)	4.59e + 01 (3.51e + 01)	2.693	0.00435
38	3.13e + 01 (2.91e + 01)	**2.13e + 01** ∗ (1.17e + 01)	2.177	0.0166
39	3.09e + 01 (2.47e + 01)	**2.06e + 01** ∗ (1.15e + 01)	2.581	0.00601
53	**1.69e + 01** ∗ (1.04e + 01)	2.32e + 01 (1.90e + 01)	2.297	0.0125
56	**1.72e + 01** ∗ (8.01e + 00)	2.40e + 01 (2.23e + 01)	2.059	0.0219
65	**1.47e + 01** ∗ (7.35e + 00)	1.90e + 01 (1.22e + 01)	2.005	0.0242
83	1.88e + 01 (1.82e + 01)	**1.23e + 01** ∗ (3.61e + 00)	2.500	0.00781
85	1.39e + 01 (6.39e + 00)	**1.16e + 01** ∗ (2.96e + 00)	2.309	0.0120
123	1.40e + 01 (1.06e + 01)	**1.07e + 01** ∗ (3.52e + 00)	2.066	0.0217
126	1.42e + 01 (1.12e + 01)	**1.08e + 01** ∗ (2.78e + 00)	2.073	0.0215
134	1.59e + 01 (1.50e + 01)	**1.04e + 01** ∗ (3.11e + 00)	2.449	0.00887
152	**1.01e + 01** ∗ (2.83e + 00)	1.17e + 01 (4.79e + 00)	1.967	0.0264
161	1.08e + 01 (4.96e + 00)	**9.17e + 00** ∗ (2.56e + 00)	2.046	0.0222
166	1.17e + 01 (5.75e + 00)	**9.46e + 00** ∗ (2.25e + 00)	2.564	0.00637
170	**9.44e + 00** ∗ (1.85e + 00)	1.40e + 01 (1.63e + 01)	1.933	0.0295
173	1.24e + 01 (8.88e + 00)	**9.83e + 00** ∗ (4.09e + 00)	1.785	0.0394
306	8.77e + 00 (2.67e + 00)	**7.86e + 00** ∗ (1.59e + 00)	1.903	0.0305
333	**7.71e + 00** ∗ (1.82e + 00)	8.80e + 00 (2.72e + 00)	2.295	0.0121
351	**7.44e + 00** ∗ (1.46e + 00)	8.11e + 00 (1.71e + 00)	1.995	0.0245
377	8.12e + 00 (1.37e + 00)	**7.57e + 00** ∗ (1.01e + 00)	2.366	0.0101

Among the entire population sizes of 20–400, 5.51% (21/381) of the results show significant discrepancy between the pair of each active-ratios at the significance level of 0.05, so as 0.262% (1/381) of the results at the significance level of 0.005, and 0.00% (0/381) of the results at the significance level of 0.0005. Here, values in **bold** show better performance that is acquired at each active ratio and they are measured in the form of mean value in respective population sizes, while each value that is denoted with asterisk is statistically significant at the significance level of 0.05 that is denoted by *, 0.005 that is denoted by **, and 0.0005 that is denoted by ***, in the one-tailed *t*-test. A value of standard deviation (S.D.), *t*-statistics, and *p*-value are provided for each value.

considered to be "necessary" can easily lead to a failure to provide an answer for understanding essentials of such system. Even for faithful reproduction the level of description should focus on the minimum requirements which are essentially associated with a limited number of target phenomena and it is advised to gradually elevate such level by including more requirements step by step (Ouellette and Gordon 2021). Analysis and visualization of the target phenomena surely demands a quantitative metrics that can represent global status of a swarm of individuals. Other metaheuristic algorithms which are categorized as decentralized methodologies don't provide a way to visually obtain validation information for grasping such global status and lacks any equivalent to global-best value provided by PSO deployed in this article.

Statistical analysis based on the discrepancy metrics has revealed that the performance simulation outcomes have been equivalent between the pair of each active-ratios of 60% and 100%. The heterogeneity of individuals that is represented by such small value of active ratio has not put any negative impacts on accomplishments of efficient swarm migration, even though it involves so large inactive population in the swarm.

Table 12. This excerpt from the complete list of the results of simulation that is performed with the shifted-Ackley's function displays the global-best value that is statistically significant.

Population Size	Global Best - Mean (S.D.)		*T*-Statistics	*P*-Value
	Active Ratio of 60%	Active Ratio of 100%		
36	**4.38e + 00** ∗ (7.91e-01)	4.74e + 00 (6.98e-01)	2.467	0.00770
37	**4.31e + 00** ∗ (7.90e-01)	4.72e + 00 (7.36e-01)	2.405	0.00905
55	**3.94e + 00** ∗ (6.34e-01)	4.20e + 00 (6.48e-01)	2.098	0.0193
56	4.06e + 00 (5.70e-01)	**3.88e + 00** ∗ (6.04e-01)	1.681	0.0480
59	4.22e + 00 (7.03e-01)	**3.96e + 00** ∗ (5.79e-01)	2.048	0.0216
60	**3.79e + 00** ∗ (7.39e-01)	4.10e + 00 (6.76e-01)	2.036	0.0222
67	4.07e + 00 (6.31e-01)	**3.82e + 00** ∗ (5.86e-01)	2.168	0.0163
76	**3.67e + 00** ∗ (5.77e-01)	3.92e + 00 (5.64e-01)	1.983	0.0251
81	3.95e + 00 (5.50e-01)	**3.68e + 00** ∗ (6.62e-01)	2.079	0.0202
89	**3.37e + 00** ∗∗ (5.78e-01)	3.70e + 00 (5.33e-01)	3.132	0.00115
101	3.58e + 00 (5.61e-01)	**3.33e + 00** ∗ (4.30e-01)	2.391	0.00939
106	**3.26e + 00** ∗∗ (5.00e-01)	3.52e + 00 (4.15e-01)	2.669	0.00447
157	3.27e + 00 (4.50e-01)	**3.10e + 00** ∗∗ (4.70e-01)	1.698	0.0464
165	3.21e + 00 (4.79e-01)	**2.95e + 00** ∗∗ (4.60e-01)	2.654	0.00466
169	**3.04e + 00** ∗∗ (4.33e-01)	3.24e + 00 (3.90e-01)	2.643	0.00480
181	**2.92e + 00** ∗ (4.83e-01)	3.15e + 00 (4.86e-01)	2.378	0.00970
189	3.07e + 00 (4.47e-01)	**2.85e + 00** ∗ (5.04e-01)	2.269	0.0127
214	**2.85e + 00** ∗ (5.21e-01)	3.06e + 00 (3.71e-01)	2.169	0.0164
222	**2.81e + 00** ∗ (5.18e-01)	3.01e + 00 (3.68e-01)	2.188	0.0157
230	3.08e + 00 (3.81e-01)	**2.82e + 00** ∗∗ (4.16e-01)	3.212	0.000897
245	**2.71e + 00** ∗ (5.57e-01)	2.95e + 00 (4.22e-01)	2.480	0.00744
247	**2.74e + 00** ∗ (4.70e-01)	2.96e + 00 (4.97e-01)	2.314	0.0114
284	2.88e + 00 (3.70e-01)	**2.70e + 00** ∗ (3.34e-01)	2.479	0.00745
289	2.85e + 00 (3.73e-01)	**2.64e + 00** ∗ (5.33e-01)	2.336	0.0109
291	**2.69e + 00** ∗ (4.44e-01)	2.87e + 00 (3.82e-01)	2.239	0.0137
329	2.79e + 00 (3.87e-01)	**2.60e + 00** ∗ (4.67e-01)	2.170	0.0162
336	**2.50e + 00** ∗ (5.14e-01)	2.73e + 00 (4.11e-01)	2.330	0.0110
340	2.74e + 00 (4.61e-01)	**2.51e + 00** ∗ (4.73e-01)	2.204	0.0149
348	2.74e + 00 (4.37e-01)	**2.50e + 00** ∗ (4.93e-01)	2.474	0.00756
351	2.67e + 00 (4.37e-01)	**2.47e + 00** ∗ (4.98e-01)	2.227	0.0142
357	**2.54e + 00** ∗ (4.68e-01)	2.77e + 00 (4.11e-01)	2.571	0.00583
364	**2.49e + 00** ∗∗ (4.34e-01)	2.73e + 00 (3.46e-01)	3.134	0.00114
387	2.65e + 00 (4.06e-01)	**2.47e + 00** ∗ (4.16e-01)	2.005	0.0239

Note: Among the entire population sizes of 20–400, 8.66% (33/381) of the results show significant discrepancy between the pair of each active-ratios at the significance level of 0.05, so as 1.84% (7/381) of the results at the significance level of 0.005, and 0.00% (0/381) of the results at the significance level of 0.0005. Here, values in **bold** show better performance that is acquired at each active ratio and they are measured in the form of mean value in respective population sizes, while each value that is denoted with asterisk is statistically significant at the significance level of 0.05 that is denoted by *****, 0.005 that is denoted by ******, and 0.0005 that is denoted by *******, in the one-tailed *t*-test. A value of standard deviation (S.D.), *t*-statistics, and *p*-value are provided for each value.

The reason for reserving such large size of inactive population has not been fully understood yet. However, it is obvious that the discussed behavioral functional-heterogeneity plays a key factor in how active worker ants manage the complex system for performing necessary tasks in swarm migration, efficiently.

This behavioral functional-heterogeneity of ground mobility is a key factor for actuating and controlling robot swarm. In the swarm, robots can have various functional heterogeneity. How many different types of robots of mobility or immobility would be built into the swarm is always a difficult problem for fulfilling implementation requirements. The discrepancy metrics with PSO used in this article is expected to provide a solution for fulfilling such

Table 13. This excerpt from the complete list of the results of simulation that is performed with the shifted-Rastrigin's function displays the global-best value that is statistically significant.

Population Size	Global Best - Mean (S.D.)		*T*-Statistics	*P*-Value
	Active Ratio of 60%	Active Ratio of 100%		
23	3.47e + 01 (8.34e + 00)	**3.04e + 01** ∗ (7.13e + 00)	2.570	0.00585
30	3.25e + 01 (8.56e + 00)	**2.78e + 01** ∗ (8.55e + 00)	2.581	0.00569
46	2.98e + 01 (7.99e + 00)	**2.61e + 01** ∗ (6.25e + 00)	2.475	0.00753
54	2.91e + 01 (7.63e + 00)	**2.47e + 01** ∗∗ (6.66e + 00)	3.319	0.000639
59	2.76e + 01 (7.69e + 00)	**2.42e + 01** ∗ (8.30e + 00)	2.015	0.0234
79	2.59e + 01 (6.27e + 00)	**2.31e + 01** ∗ (6.78e + 00)	2.251	0.0133
105	**2.03e + 01** ∗ (5.39e + 00)	2.29e + 01 (6.03e + 00)	2.381	0.00962
145	2.14e + 01 (5.54e + 00)	**1.88e + 01** ∗ (5.89e + 00)	1.989	0.0248
155	**1.95e + 01** ∗ (6.74e + 00)	2.21e + 01 (5.72e + 00)	2.096	0.0193
159	2.29e + 01 (7.19e + 00)	**1.96e + 01** ∗ (6.71e + 00)	2.570	0.00585
163	**2.00e + 01** ∗ (5.95e + 00)	2.25e + 01 (5.70e + 00)	2.224	0.0143
167	2.00e + 01 (6.94e + 00)	**1.80e + 01** ∗ (5.27e + 00)	1.742	0.0424
176	**1.85e + 01** ∗ (6.01e + 00)	2.10e + 01 (5.56e + 00)	2.252	0.0133
182	2.17e + 01 (5.97e + 00)	**1.87e + 01** ∗ (6.42e + 00)	2.396	0.00927
200	**1.82e + 01** ∗ (5.90e + 00)	2.08e + 01 (5.98e + 00)	2.281	0.0124
204	**1.68e + 01** ∗ (5.39e + 00)	1.95e + 01 (6.16e + 00)	2.191	0.0154
208	**1.73e + 01** ∗ (4.59e + 00)	2.00e + 01 (6.79e + 00)	2.427	0.00866
215	2.12e + 01 (4.96e + 00)	**1.89e + 01** ∗ (4.47e + 00)	2.011	0.0236
228	**1.54e + 01** ∗ (4.87e + 00)	1.80e + 01 (6.71e + 00)	2.266	0.0130
250	1.86e + 01 (3.94e + 00)	**1.65e + 01** ∗ (5.32e + 00)	2.449	0.00812
299	**1.73e + 01** ∗ (5.23e + 00)	1.95e + 01 (5.46e + 00)	1.896	0.0305
301	**1.59e + 01** ∗ (5.70e + 00)	1.81e + 01 (4.73e + 00)	2.424	0.00861
305	1.80e + 01 (5.67e + 00)	**1.58e + 01** ∗ (4.49e + 00)	1.858	0.0331
306	**1.61e + 01** ∗ (5.63e + 00)	1.90e + 01 (5.74e + 00)	2.514	0.00681
345	1.77e + 01 (5.27e + 00)	**1.50e + 01** ∗ (4.30e + 00)	2.550	0.00617
367	**1.49e + 01** ∗ (4.87e + 00)	1.69e + 01 (4.65e + 00)	1.950	0.0271
376	1.70e + 01 (6.01e + 00)	**1.46e + 01** ∗ (4.85e + 00)	2.060	0.0210
393	1.80e + 01 (4.90e + 00)	**1.56e + 01** ∗ (4.86e + 00)	2.550	0.00618
394	1.74e + 01 (5.32e + 00)	**1.55e + 01** ∗ (4.42e + 00)	1.967	0.0260

Among the entire population sizes of 20–400, 7.61% (29/381) of the results show significant discrepancy between the pair of each active-ratios at the significance level of 0.05, so as 0.262% (1/381) of the results at the significance level of 0.005, and 0.00% (0/381) of the results at the significance level of 0.0005. Here, values in **bold** show better performance that is acquired at each active ratio and they are measured in the form of mean value in respective population sizes, while each value that is denoted with asterisk is statistically significant at the significance level of 0.05 that is denoted by *, 0.005 that is denoted by **, and 0.0005 that is denoted by ***, in the one-tailed *t*-test. A value of standard deviation (S.D.), *t*-statistics, and *p*-value are provided for each value.

implementation requirements by selecting different types of robots comprising the swarm and minimizing the discrepancy of performance between them, visually.

The next section provides conclusions of this article and a direction to explore our future work.

6. Conclusions

This article showed emulation of the extreme heterogeneity of ground mobility between individuals of *Temnothorax albipennis* ant species by using the classical metaheuristic algorithm, PSO, with a set of simple parameter configurations. A concept of discrepancy was used for providing a quantitative metrics based on performance simulation outcomes of the algorithm in order to visualize the influence of heterogeneity of individuals on global status of swarm migration.

Using statistical testing, we confirmed that the emulation with the algorithm was successful even with a comparison between a pair of specific active-ratios. PSO depends on not only local information gathering but also global information integration based on global-best positions. As a countermeasure, the discussed phenomena could be faithfully reproduced by using other decentralized algorithms such as ant colony optimization algorithms, bat algorithms, differential evolution algorithms. However, it was established that lack of global information integration makes it impossible to create visualization of global status of the target swarm with reliable quantitative statistical-analysis. In the emulation, our choice of PSO is one of the best solutions for visualizing the influence of heterogeneity of individuals on global status of swarm migration at the present. In addition, it is necessary to detect global-best positions of a swarm obtained from the iterative steps in order to provide a technical solution for accurate and simultaneous control and visual monitoring of robot swarm migration. Unfortunately, the emulation executed in this article does not focus on improving the computing time of algorithms. However, in our future work, we will investigate whether integration of other metaheuristic algorithms contributes to acceleration of performance simulation process. Furthermore, visualization provides the basis for evaluation of global status of swarm migration and it is expected to lead to exploration of robot swarm migration involving various functional heterogeneity of ground mobility. Our study can be considered as a step to advance algorithm formulation in order to build a bridge advancing toward a direction of swarm robotics-oriented research.

Disclosure statement

No potential conflict of interest was reported by the author.

ORCID

Hideyasu Sasaki http://orcid.org/0000-0002-2821-0857

Data availability statement

The raw data supporting the conclusions of this article will be made available by the author, without undue reservation.

References

Aguilar, J., Monaenkova, D., Linevich, V., Savoie, W., Dutta, B., Kuan H. S., Betterton M D., Goodisman, M. A. D., & Goldman, D I. 2018. Collective clog control: Optimizing traffic flow in confined biological and robophysical excavation. *Science 361* (6403):672–77. doi:10.1126/science.aan3891.

Aina, K. O, Avinery, R., Kuan H. S., Betterton, M. D., Goodisman, M. A. D. & Goldman, D. I. 2022. Capable active matter: Learning to avoid clogging in confined collectives via collisions. *Frontiers in Physics 10*:735667. doi:10.3389/fphy.2022.735667.

Camazine, S., Deneubourg, J. L., Franks, N. R., Sneyd, J., Theraulaz, G., & Bonabeau, E. 2001. *Self-organization in biological systems*. Princeton, NJ: Princeton Univ. Press.

Charbonneau, D., Sasaki, T., & Dornhaus, A. 2017. Who needs 'lazy' workers? Inactive workers act as a 'reserve' labor force replacing active workers, but inactive workers are not replaced when they are removed. *Public Library of Science (PLoS) 12* (9):0184074. doi:10.1371/journal.pone.0184074.

Chowdhury, D., Guttal, V., Nishinari, K., & Schadschneider, A. 2002. A cellular-automata model of flow in ant trails: Non-monotonic variation of speed with density. *Journal of Physics A: Mathematical and Theoretical 35* (41):573–77. doi:10.1088/0305-4470/35/41/103.

Cleghorn, C. W., & Engelbrecht, A. P. 2018. Particle swarm stability: A theoretical extension using the non-stagnate distribution assumption. *Swarm Intelligence 12* (1):1–22. doi:10.1007/s11721-017-0141-x.

Clerc, M., & Kennedy, J. 2002. The particle swarm - explosion, stability, and convergence in a multidimensional complex space. *IEEE Transactions on Evolutionary Computation 6* (1):58–73. doi:10.1109/4235.985692.

Dorigo, M., Floreano, D., Gambardella, L. M., Mondada, F., Nolfi, S., Baaboura, T., Birattari, M., Bonani, M., Brambilla, M., Brutschy, A., et al. 2013. Swarmanoid: A novel concept for the study of heterogeneous robotic swarms. *IEEE Robotics & Automation Magazine 20* (4):60–71. doi:10.1109/MRA.2013.2252996.

Dorigo, M., Theraulaz, G., & Trianni, V. 2021. Swarm robotics: Past, present, and future. *Proceedings of the IEEE 109* (7):1152–65. doi:10.1109/JPROC.2021.3072740.

Dornhaus, A., Holley, J. A., & Franks, N. R. 2009. Larger colonies do not have more specialized workers in the ant *Temnothorax albipennis*. *Behavioral Ecology 20* (5):922–29. doi:10.1093/beheco/arp070.

Dornhaus, A., Holley, J. A., Pook, V. G., Worswick, G., & Franks, N. R. 2008. Why do not all workers work? Colony size and workload during emigrations in the ant *Temnothorax albipennis*. *Behavioral Ecology and Sociobiology 63* (1):43–51. doi:10.1007/s00265-008-0634-0.

Garnier, S., Jost, C., Gautrais, J., Asadpoury, M., Caprari, G., Jeanson, R., Grimal A., & Theraulaz, G. 2008. The embodiment of cockroach aggregation behavior in a group of micro-robots. *Artificial Life 14* (4):387–408. doi:10.1162/artl.2008.14.4.14400.

Geraghty, M. J., Dunn, R. R., & Sanders, N. J. 2007. Body size, colony size, and range size in ants (*Hymenoptera*: *Formicidae*): Are patterns along elevational and latitudinal gradients consistent with Bergmann's rule? *Myrmecological News 10*:51–58.

Gravish, N., Garcia, M., Mazouchova, N., Levy, L., Umbanhowar, P. B., Goodisman, M. A. D., & Goldman, D. I. 2012. Effects of worker size on the dynamics of fire ant tunnel construction. *Journal of the Royal Society Interface 9* (77):3312–22. doi:10.1098/rsif.2012.0423.

Gravish, N., Gold, G., Zangwill, A., Goodisman, M. A. D., & Goldman, D. I. 2015. Glass-like dynamics in confined and congested ant traffic. *Soft Matter 11* (33):6552–61. doi:10.1039/c5sm00693g.

John, A., Schadschneider, A., Chowdhury, D., & Nishinari, K. 2008. Characteristics of ant-inspired traffic flow: Applying the social insect metaphor to traffic models. *Swarm Intelligence 2* (1):25–41. doi:10.1007/s11721-008-0010-8.

John, A., Schadschneider, A., Chowdhury, D., & Nishinari, K. 2009. Traffic like collective movement of ants on trails: Absence of jammed phase. *Physical Review Letters 102* (10):108001. doi:10.1103/PhysRevLett.102.108001.

Kennedy, J. 2003. Bare bones particle swarms. In Proceedings of the 2003 IEEE International Symposium on Swarm Intelligence, 80–87. IEEE Press, Piscataway, NJ. doi:10.1109/SIS.2003.1202251.

Kennedy, J., & Eberhart, R. 1995. Particle swarm optimization. In Proceedings of the 1995 IEEE International Conference on Neural Networks, 1942–48. IEEE Press, Piscataway, NJ. doi:10.1109/ICNN.1995.488968.

Linevich V., Monaenkova, D., & Goldman, D. I. 2016. Robophysical study of excavation in confined environments. *Artificial Life and Robotics 21* (4):460–65. doi:10.1007/s10015-016-0317-2.

Li, X., Tang, K., Omidvar, M. N., Yang, Z., & Qin, K. 2013. *Technical report: Benchmark functions for the CEC'2013 special session and competition on large scale global optimization*. Melbourne, Australia: Evolutionary computation and machine learning group, RMIT University. https://titan.csit.rmit.edu.au/e46507/cec13-lsgo/competition/cec2013-lsgo-benchmark-tech-report.pdf.

Miranda, L. J. V. 2019. *PySwarms a research toolkit for Particle Swarm Optimization in Python*. https://pyswarms.readthedocs.io/en/latest/.

Monaenkova, D., Gravish, N., Rodriguez, G., Kutner, R., Goodisman, M. A. D., & Goldman, D. I. 2015. Behavioral and mechanical determinants of collective subsurface nest excavation. *The Journal of Experimental Biology 218* (9):1295–305. doi:10.1242/jeb.113795.

Ouellette, N. T., & Gordon, D. M. 2021. Goals and limitations of modeling collective behavior in biological systems. *Frontiers in Physics 9*:687823. doi:10.3389/fphy.2021.687823.

Pereira, G. 2010. *Particle swarm optimization in artificial life by example*. http://web.ist.utl.pt/gdgp/VA/pso.htm.

Pratt, S. C. 2005. Behavioral mechanisms of collective nest-site choice by the ant *Temnothorax curvispinosus*. *Insectes Sociaux 52* (4):383–92. doi:10.1007/s00040-005-0823-z.

Rauf, H. T., Bangyal, W. H. K., & Lali, M. I. 2021. An adaptive hybrid differential evolution algorithm for continuous optimization and classification problems. *Neural Computing & Applications 33* (17):10841–67. doi:10.1007/s00521-021-06216-y.

Rauf, H. T., Malik, S., Shoaib, U., Irfan, M. N., & Lali, M. I. 2020. Adaptive inertia weight Bat algorithm with Sugeno-function fuzzy search. *Applied Soft Computing 90*:106159. doi:10.1016/j.asoc.2020.106159.

Sasaki, H. 2019a. Modeling ant nest relocation at low active ratio by particle swarm optimization. In Proceedings of the 21st IEEE Congress on Evolutionary Computation, 594–603. IEEE Press, Piscataway, NJ. doi:10.1109/CEC.2019.8789942.

Sasaki, H. (2019b). Modeling fast and robust ant nest relocation using particle swarm optimization. In Proceedings of the 2019 Conference on Artificial Life, 626–33. The MIT Press, Cambridge, MA. doi:10.1162/isal_a_00231.

Sasaki, H., & Leung, H. 2013. Trail traffic flow prediction by contact frequency among individual ants. *Swarm Intelligence 7* (4):307–26. doi:10.1007/s11721-013-0085-8.

Yarpiz Team. 2015. Particle swarm optimization in MATLAB. In *Yarpiz - Academic Source Codes and Tutorials*. http://yarpiz.com/50/ypea102-particle-swarm-optimization